

SOI-Based 3dB MMI Splitter^{*}

WEI Hong-zhen(魏红振)¹, YU Jin-zhong(余金中)¹, LIU Zhong-li(刘忠立)²,
ZHANG Xiao-feng(张晓峰)¹, SHI Wei(史 伟)³ and FANG Chang-shui(房昌水)³

(1 State Key Laboratory on Integrated Optoelectronics, Institute of Semiconductors,
The Chinese Academy of Sciences, Beijing 100083, China)

(2 Microelectronics Center, Institute of Semiconductors, The Chinese Academy of Sciences, Beijing 100083, China)

(3 State Key Laboratory of Crystal Materials, Shandong University, Jinan 250100, China)

Abstract: A type of SOI-based MMI 3dB splitter has been demonstrated. The geometry was analyzed and designed by effective index method and guide mode method. The fabrication tolerance was analyzed too. The device was fabricated and near-field output was obtained. The device shows large width tolerance, low loss and low power uniformity.

Key words: SOI; multimode interference; integrated optics

PACC: 4282

CLC number: TN256 **Document code:** A **Article ID:** 0253-4177(2000)11-1055-05

1 Introduction

3dB splitter is one of the key devices in the integrated optics. Y-branch and X-cross branch are both the conventional structures to realize 3dB splitter, however, which are difficult to fabricate because of the small branch angle. In recent years, MultiMode Interference (MMI) couplers, based on the self-imaging effect, are accepted popularly due to their advantages, such as low-loss, compact size and large fabrication tolerance^[1,2]. Couplers based on MMI structure can be obtained in various materials, such as InP, SiO₂, and GaAs. Their excellent performance has been reported^[3-5]. Silicon-On-Insulator (SOI) technology is considered being a promising technology to guide wave photonic devices operating in the infrared ($\lambda > 1.2\mu\text{m}$). The SOI-CMOS integrated circuit, being the future low-power, high-speed electronic technology, ensures the availability of high-quality low-cost substrates. Because of the large index step between Si and SiO₂ ($\Delta n \sim 2.0$), thin cladding layer ($< 1.0\mu\text{m}$) is used in SOI waveguide structures, making them compatible

* Project Supported by National Natural Science Foundation of China Under Grant No. 69896260 and 69990540.

WEI Hong-zhen (魏红振) was born in 1969. He is currently a Ph. D. candidate. His research interests are in integrated optoelectronics devices. E-mail: weihz@red.semi.ac.cn

Received 15 March 2000, revised manuscript received 24 April 2000

with VLSI technology. In contrast to the silica waveguide technology, 5–10 μm thick cladding cover layer is needed due to the low index step. Therefore, development of optical and optoelectronic devices in SOI technology makes it possible to fabricate low-cost, monolithic optoelectronics circuits. In this letter, we present the design, performance analysis and fabrication of integrated 1×2 3dB MMI splitter with SOI technology. The fabrication tolerance is also analyzed. The process technology is fully compatible with the silicon CMOS integrated circuit process.

2 Design

An MMI coupler is based on the self-imaging property of a multimode waveguide. Schematic diagram of the 3dB MMI splitter is shown in Fig. 1. The MMI splitter consists of a single mode input waveguide, a planar multimode waveguide and two single-mode output waveguides. Because of the large index step of Si and SiO_2 , the rib structure should be applied to the SOI waveguides to load the fundamental mode under a certain condition^[6]. Schematic of the rib SOI waveguide is shown in Fig. 2.

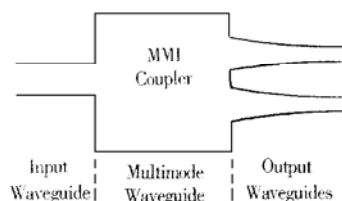


FIG. 1 Schematic Diagram of 1×2 MMI Splitter

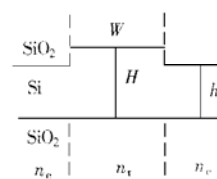


FIG. 2 Schematic Diagram of SOI Rib Waveguide

In the MMI splitter, fundamental mode field is fed into the multimode waveguide at the center. In this situation, only even symmetric modes are excited. The imaging in the multimode waveguide is obtained by linear combinations of the even symmetric modes. To form two-fold images, the length of the multimode waveguide should be^[7]:

$$L = \frac{p n_r W_{\text{eff}}^2}{2\lambda} \quad (1)$$

where p indicates the imaging periodicity. For the shortest device, $p = 1$. W_{eff} is the effective width of the multimode waveguide, n_r is the refractive index of the multimode section, λ is the free space wavelength of the light. The two output waveguides are symmetrically located with equal spacing width.

A simple method to simulate the MMI devices is the effective index method or the guide-mode method. The simulated images in the multimode waveguide at the distance determined by formula (1) are shown in Fig. 3. The width of the multimode waveguide is 40 μm . Heights of the inner and outer rib are 10 μm and 6 μm respectively. The corresponding length of the multimode waveguide is 2713 μm . In principle, three guide modes can form two-fold images in the multimode waveguide. However, simulating result shows that

with the guide modes increasing, the images become narrow and the loss and crosstalk of the device reduce. So large confinement, which is the deep etching of the rib guides, is useful to enhance the performance of the device. However, the etching depth of the guides is limited by the single mode condition of the access guides. The simulation result also shows that the widths of the output waveguides have important influence on the characteristics of the MMI coupler. With the widths increasing, the loss and power uniformity of the splitter reduced. Tapered waveguides were used to connect the multimode waveguide and the access waveguides, as shown in Fig. 1.

One of the main advantages of the MMI device is the large fabrication tolerance. Fabrication tolerances refer to the control of the geometrical dimensions during processing and its subsequent impact on device performance. From formula (1), it is obvious that the multimode section width is by far the most critical parameter to be controlled during the fabrication. Tolerance can be evaluated by the influence of a small change in the dimension on the loss and power uniformity of the MMI device. Loss can be evaluated by overlapping the imaging field with the output waveguide mode field. The power uniformity is determined by:

$$UF = 10\log(P_1/P_2) \quad (2)$$

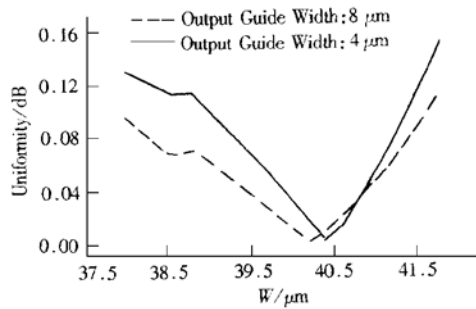


FIG. 4 Tolerance of MMI Splitter to Width of Multimode Waveguide

wider access waveguides. Tapered waveguides are used to connect the multimode waveguide with the access guides, as shown in Fig. 1.

3 Fabrication

The conventional Si process technology is used to fabricate the MMI splitter. The SIMOX SOI wafer with buried SiO₂ and top silicon being both 0.25 μm was followed by 11 μm of the epitaxial monocrystal silicon. The rib waveguides and MMI splitters were

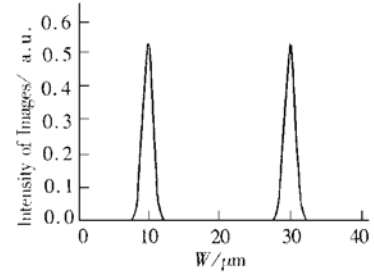


FIG. 3 Simulated Images of 1×2 MMI Splitter Multimode
Width: $W = 40\mu\text{m}$, Length: $L = 2713\mu\text{m}$

where P_1 and P_2 ($P_1 > P_2$) are the output power in the two branches respectively. The simulated tolerance of the width of the multimode section is shown in Fig. 4. Length of the multimode section is 2713 μm. Heights of the inner and outer rib are 10 and 6 μm respectively. The simulated result shows that the width tolerance of the MMI splitter can be relaxed greatly by using wider output waveguides. In general, for a given wavelength and technology, all tolerance can be relaxed by using

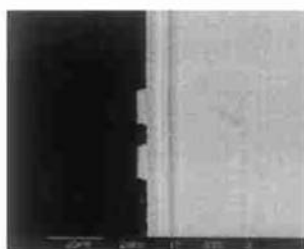


FIG. 5 SEM Graph of Output Facet of MMI Splitter

formed by one-step RIE (Reactive Ion Etching) processing using a Cr mask. The etching was performed at 3 sccm SF_6 and 10 sccm N_2 with 100W RF power of 30 min. In our design, the widths of the access waveguides were $10\mu\text{m}$, and several splitters with different dimension size were designed to evaluate the tolerance. The lengths of the multimode section in these splitters are $2713\mu\text{m}$. Widths of the multimode section are 39, 40, 41 and $42\mu\text{m}$, respectively. Correspondingly, the splitter samplers were numbered 1[#], 2[#], 3[#] and 4[#]. The rib etching depth is $5\mu\text{m}$ throughout the chip. The SEM graph of the output waveguide facet is shown in Fig. 5. The top cladding layer was formed by a dry-wet-dry thermal oxidation on the patterned SOI wafer. Thickness of the cover SiO_2 is about $0.7\mu\text{m}$. So, the thickness of the core-layer of the inner rib section is about $10.5\mu\text{m}$. Tapered waveguides were used to connect the multimode section with the output waveguide. The wafer was thinned and cleaved.

4 Experimental Result

The light from the fiber at wavelength $\lambda = 1.3\mu\text{m}$ was coupled into the rib waveguides through the cleaved facet of an input guide. The light emerging from the output waveguides was projected onto the light sensitive area of an infrared CCD using a $\times 20$ microscope objective. Then the image was displayed on the TV monitor with a total 200 magnification of that of the cleaved output facet. The CCD had a line scan facility, which was used to measure the intensity profiles through the center of the output spots, by which we can estimate the power uniformity of the coupler. The images on TV were taken by a digital camera. Figure 6 shows the measured near-field images of each output waveguides of sample 4[#]. The measured result of sample 1[#], 2[#] and 3[#] are the same as that of the sample 4[#]. There is no obvious different results for different sample. The result shows that the width tolerance of the MMI device is large enough for the conventional Si process technology. Not including the reflective loss of the two facets, the excess loss of sample 4[#] is about 1.8dB. The power uniformity of the two output branches is less than 0.5dB.



FIG. 6 Measured Near-Field Image of Two Output Waveguides in MMI Splitter (Sample 4[#])

5 Conclusion

In conclusion, we have demonstrated the 3dB MMI splitter based on SOI in a form suitable for the OEIC application. The splitter with different width of multimode section were designed and fabricated. The output near-field images were obtained. The excess loss

of the splitter is about 1.8dB. The power uniformity is less than 0.5dB. The width tolerance of device is enough large for conventional Si process technology.

References

- [1] M. A. Fardad and M. Fallahi, IEEE Photonics Technol. Lett., 1999, **11**(6): 697—699.
- [2] Mohammad R. Paian and Robert I. MacDonald, Appl. Opt., 1997, **36**(21): 5097—5108.
- [3] Pierre A. Besse, Maurus Bachmann, H. Melchior, L. B. Soldano and M. K. Smit, J. Lightwave Technol., 1994, **12**(6): 1004—1009.
- [4] R. M. Jerkins, J. M. Heaton, D. R. Wight, J. T. Parker, J. C. H. Birbeck and G. W. Smith, Appl. Phys. Lett., 1994, **64**(6): 684—686.
- [5] Q. Lai, M. Bachmann, W. Hunziker, P. A. Besse and H. Melchior, Electron. Lett., 1996, **32**(17): 1576—1577.
- [6] R. A. Soref, J. Schmidtchen and K. Petermann, IEEE J. Quantum Electron., 1997, **27**: 1971—1973.
- [7] Lucas. B. Soldano and Erik C. M. Pennings, J. Lightwave Technol., 1995, **13**(4): 615—627.